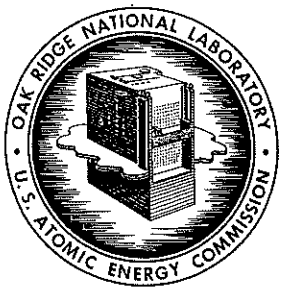

OAK RIDGE NATIONAL LABORATORY
operated by
UNION CARBIDE CORPORATION
for the
U.S. ATOMIC ENERGY COMMISSION

ORNL - TM - 1274

168

A MODEL FOR FISSION PRODUCT TRANSPORT AND DEPOSITION UNDER ISOTHERMAL CONDITIONS

T. S. Kress
F. H. Neill

ORNL-TM-1274

Contract No. W-7405-eng-26

REACTOR DIVISION

A MODEL FOR FISSION PRODUCT TRANSPORT AND DEPOSITION UNDER ISOTHERMAL CONDITIONS

T. S. Kress
F. H. Neill

For Presentation at
The American Society of Mechanical Engineers
Nuclear Engineering Division

Winter Annual Meeting
November 7-11, 1965
Chicago, Illinois

OCTOBER 1965

OAK RIDGE NATIONAL LABORATORY
Oak Ridge, Tennessee
operated by
UNION CARBIDE CORPORATION
for the
U.S. ATOMIC ENERGY COMMISSION

TABLE OF CONTENTS

A MODEL FOR FISSION PRODUCT TRANSPORT AND DEPOSITION UNDER ISOTHERMAL CONDITIONS*

T. S. Kress
F. H. Neill

ABSTRACT

The transport of fission products through a carrier coolant stream and their deposition onto the conduit surfaces have been studied analytically and experimentally. The model developed assumes validity of the heat-mass analogy under conditions of radioactive decay and an imperfect sink that may saturate and postulates a classical adsorption-desorption interaction at the conduit surface.

Mass balances in the carrier stream and on the conduit surface result in a set of time-dependent, nondimensional differential equations. These equations express the concentration in the gas stream and on the conduit surface as functions of time, axial position, and the identified fission product deposition parameters.

Equilibrium solutions are presented along with transient solutions of a limiting condition of the equations shown to be equivalent to a set in the literature.

The experimental facility, built to observe out-of-pile deposition, basically contains an isothermal helium circulating loop, provisions for installing different test sections, and a system for injecting a variety of radioactive isotopes at rates simulating release from reactor fuel. Results for the deposition of iodine on low carbon and stainless steel are presented and compared with the theory.

INTRODUCTION

As operating temperatures are extended to higher levels in gas-cooled reactors, retaining fission products within the fuel elements becomes increasingly difficult. Complete or controlled release of fission products

---

*The model presented in this report was abstracted from a thesis submitted by T. S. Kress to the University of Tennessee as partial fulfillment for a Master of Science degree from the Mechanical and Aerospace Engineering Department.

appears desirable for some reactor concepts. An optimization of the degree of retention requires evaluating the cost penalty associated with maintaining primary coolant systems with varying degrees of contamination. However, not enough is known about the transport and deposition of fission products to determine the amount and distribution of this contamination.

Previous investigations (1,2,3,4,5,6,7)[1] have described the transport of fission products in a reactor carrier stream by traditional convection and concentration gradient diffusion equations. Only limited success has been achieved in introducing a phenomenological wall factor to account for interactions at the conduit surface (1,5). The present investigation assumes validity of the heat-mass analogy under conditions of radioactive decay (2) and an imperfect sink that may saturate, postulates an adsorption-desorption interaction at the surface,[2] arrives at relations for predicting transport and deposition of fission-products, identifies the parameters involved, and presents experimental data that agree well with the predictions. The complicating factors of precursors, higher order surface reactions, chemical reactions among elements, diffusion under a thermal gradient, competition among fission products for deposition surfaces, presence of particulate size matter, recirculation of the depositing species in a closed circuit, surface mobility, and diffusion into the walls of the conduit were not included.

---

[1] Numbers in parenthesis refer to similarly numbered references in bibliography at end of paper.

[2] After the development of the present model, it was learned that this mechanism was previously proposed in an excellent report by Epstein and Evans (12). However, the present model is shown to reduce to the Epstein and Evans equations only as a limiting case.

FISSION PRODUCT TRANSPORT AND DEPOSITION MODEL

Typically, deposition of fission products decreases exponentially in the direction of flow away from the source but is locally higher at entrance regions and regions of flow perturbations (6). This behavior is highly suggestive of mass transfer across a concentration potential with axial depletion of the concentration. The transport through the carrier stream, then, is considered to be by axial convection and radial turbulent diffusion. On reaching the conduit surface, molecules undergo an interaction with the surface material often classified as being either chemisorption (8) or physical adsorption (9). In many of these interactions, there is an exchange in which molecules are continually being both adsorbed on and desorbed from the surface. An Arrhenius type equation adequately describes the desorption rate for most physical bonds and many chemical bonds as well (10). The rate of desorption for fission products then is assumed to be given by[3]

$$\frac{\partial M}{\partial t} \cong - \theta M \qquad [1]$$

where $\theta = \omega \exp (- Q/RT)$. [2]

Desorbed molecules are assumed to "thermalize" in a very narrow region of thickness δ (a few mean-free-paths) near the surface where the carrier stream velocity is essentially zero. This assumption allows fission-product deposition to be treated in the same manner as the many adsorption isotherms (9). Because of its wide applicability and simplicity, Langmuir's classical adsorption relation is used in which the number of molecular collisions per unit surface area is expressed from the kinetic theory of gases simply as

$$p(2\pi RTm/g_c)^{-1/2} ,$$

[3] Terms are defined in Nomenclature at end of paper.

In terms of the average concentration, $\overline{N}_\delta$, in the region δ, the gross collision rate per unit area for a perfect gas equation of state is

$$\overline{N}_\delta (RTg_c/2\pi m)^{1/2} .$$

Molecules are assumed to adsorb only on "bare" surface which decreases proportionally as the surface becomes covered or as the surface concentration, M, approaches a maximum, M_s. Further, only a fraction, σ, of the "bare" surface is assumed acceptable (or preferred) for adsorption. Therefore, the adsorption rate per unit of geometrical surface area is

$$\sigma Kr \overline{N}_\delta (1 - M/M_s)$$

where $Kr \equiv (RTg_c/2\pi m)^{1/2}$.

The analogy between heat and mass transfer has been demonstrated analytically to be valid under many flow conditions involving radioactive decay (1). In addition, the analogy is assumed to remain valid as the surface saturates or as deposition approaches an equilibrium. Therefore, mass balancing in the bulk carrier stream, in the region δ, and on the conduit surface gives respectively:

$$\frac{\partial \overline{N}}{\partial t} + \overline{U}_x \frac{\partial \overline{N}}{\partial x} + \lambda \overline{N} + \frac{4h}{D} (\overline{N} - \overline{N}_\delta) = 0 , \qquad [3]$$

$$\delta \left(\frac{\partial \overline{N}_\delta}{\partial t} + \lambda \overline{N}_\delta \right) - h(\overline{N} - \overline{N}_\delta) - \theta M + \sigma \overline{N}_\delta (Kr) (1 - M/M_s) = 0 , \qquad [4]$$

and

$$\frac{\partial M}{\partial t} - \sigma (Kr) (1 - M/M_s) \overline{N}_\delta + M(\theta + \lambda) = 0 . \qquad [5]$$

The somewhat heuristic δ was introduced merely as an expediency to make use of existing surface chemistry relations. One would expect δ to be very small. Therefore, the influence of the first term in Eq. 4 will not be great, especially after deposition has progressed toward a steady state. Neglecting the first term effectively removes δ from the model, and Eq. 4 is solved for $\overline{N}_\delta$ to give

$$\overline{N}_\delta = \left[\frac{(h\overline{N} + \theta M)}{h + \sigma Kr (1 - M/M_s)} \right] . \qquad [6]$$

On substitution of Eq. 6, Eqs. 3 and 5 become respectively:

$$\frac{\partial \overline{N}}{\partial t} + \overline{U}_x \frac{\partial \overline{N}}{\partial x} + \left\{ \lambda + \frac{4h}{D} - \frac{4h^2}{D\,[h + \sigma Kr(1 - M/M_s)]} \right\} \overline{N} - \left\{ \frac{4h\theta}{D\,[h + \sigma Kr(1 - M/M_s)]} \right\} M = 0 \ . \qquad [7]$$

$$\frac{\partial M}{\partial t} + \left\{ \theta + \lambda - \frac{\sigma Kr(1 - M/M_s)\theta}{[h + \sigma Kr(1 - M/M_s)]} \right\} M - \left\{ \frac{h\sigma Kr(1 - M/M_s)}{[h + \sigma Kr(1 - M/M_s)]} \right\} \overline{N} = 0 \ . \qquad [8]$$

For a uniform source, $\overline{N}_o$, at $x = 0$, Eqs. 7 and 8 may be expressed in nondimensional form as

$$\frac{\partial \overline{N}_*}{\partial t_*} + \frac{U_*}{D_*} \frac{\partial \overline{N}_*}{\partial x_*} + \left\{ \lambda_* + \frac{4h_*}{D_*} - \frac{4h_*^2}{D_*[h_* + \sigma Kr_*(1 - M/M_{s*})]} \right\} \overline{N}_* - \left\{ \frac{4h_*\theta_*}{D_*[h_* + \sigma Kr_*(1 - M_*/M_{s*})]} \right\} M_* = 0 \ , \qquad [9]$$

and

$$\frac{\partial M_*}{\partial t_*} + \left\{ \theta_* + \lambda_* - \frac{\theta_*\sigma Kr_*(1 - M_*/M_{s*})}{[h_* + {}_\sigma Kr_*(1 - M_*/M_{s*})]} \right\} M_* - \left\{ \frac{h_*\sigma Kr_*(1 - M_*/M_{s*})}{[h_* + \sigma Kr_*(1 - M_*/M_{s*})]} \right\} \overline{N}_* = 0 \ , \qquad [10]$$

in which the following dimensionless quantities have been defined:

$$x_* = x/D \qquad t_* = t(\tau_w g_c/\mu)$$

$$D_* = D\sqrt{\tau_w g_c/\rho}\,/\upsilon \qquad \theta_* = \theta/(\tau_w g_c/\mu)$$

$$U_* = \overline{U}_x/\sqrt{\tau_w g_c/\rho} \qquad \lambda_* = \lambda/(\tau_w g_c/\mu)$$

$$\overline{N}_* = \overline{N}/\overline{N}_o \qquad h_* = h/\sqrt{\tau_w g_c/\rho}$$

$$M_* = M\sqrt{\tau_w g_c/\rho}\,/\overline{N}_o\upsilon \qquad Kr_* = (RTg_c/2\pi m)^{1/2}\,/\sqrt{\tau_w g_c/\rho} \ .$$

$$M_{s*} = M\sqrt{\tau_w g_c/\rho}\,/\overline{N}_o\upsilon$$

Equations 9 and 10 with appropriate boundary conditions represent the simplified model proposed. The parameters may be identified by introducing the Blasius friction coefficient, C_f, defined by

$$\tau_w = C_f \rho \bar{U}_x^2 / g_c \ .$$

The following relations may then be determined:

$$U_* = 1 \sqrt{C_f} \ , \qquad [11]$$

$$D_* = \sqrt{C_f}\, N_{Re} \ , \qquad [12]$$

and

$$U_*/D_* = 1/(C_f\, N_{Re}) \ . \qquad [13]$$

In addition, the dimensionless mass transfer coefficient, h_*, may usually be established by analogy in terms of dimensionless parameters for a given regime of flow. An example for fully developed turbulent flow is (11)

$$h_* = \frac{\sqrt{C_f}}{[1 + 1.5\, N_{Re}^{-1/8}\, N_{Sc}^{-1/6}\, (N_{Sc} C_f / C_{fo} - 1)]} \ , \qquad [14]$$

where C_{fo} is the friction coefficient for a smooth surface (e.g., $C_{fo} = 0.316/8 N_{Re}^{1/4}$), and C_f is the usual function of N_{Re} and the relative roughness, k_*. Inspection of Eqs. 9 through 14 reveals that the fission-product deposition parameters based on this model are θ_*, λ_*, σKr_*, M_{s*}, N_{Re}, N_{Sc}, and k_*.

The equilibrium solution to Eqs. 9 and 10 is readily obtained by direct integration (see Appendix). For non-radioactive species ($\lambda = 0$), the equilibrium solution reduces to

$$(1 - M_*/M_{s*})/M_* = \theta_*/\sigma Kr_* \qquad [15]$$

which, of course, is equivalent to Langmuir's adsorption isotherm. This result is of particular interest not only for its utility but it indicates that the equilibrium solution for a convecting system approaches that of a static system if desorbed molecules do not travel far into the convection stream. This conclusion should be of particular interest to reactor designers who may be concerned with the contamination resulting from long-lived fission products and long term reactor operation. By establishing the surface chemistry of fission-product mixtures through systematic static tests, then the limiting contamination levels for actual operation under flow conditions can be readily calculated.

For the condition of low surface coverage, $M_*/M_{s*} << 1$, Eqs. 9 and 10 reduce to

$$\frac{\partial \bar{N}_*}{\partial t_*} + \frac{U_*}{D_*}\frac{\partial \bar{N}_*}{\partial x_*} + \left[\lambda_* + \frac{4h_*}{D_*} - \frac{4h_*^2}{D_*(h_* + \sigma Kr_*)}\right]\bar{N}_* - \left[\frac{4h_*\theta_*}{D_*(h_* + \sigma Kr_*)}\right] M_* = 0 \ , \quad [16]$$

and

$$\frac{\partial M_*}{\partial t_*} + \left[\theta_* + \lambda_* - \frac{\sigma Kr_*\theta_*}{(h_* + \sigma Kr_*)}\right] M_* - \left[\frac{\sigma Kr_* h_*}{(h_* + \sigma Kr_*)}\right]\bar{N}_* = 0 \ . \quad [17]$$

These are equivalent to a pair given by Epstein and Evans (12) for which they present an analytical solution (13) repeated below in terms of the present nomenclature:

for $t_* < x_* D_*/U_*$; $\quad M_* = \bar{N}_* = 0$,

for $t_* > x_* D_*/U_*$, and $M_*/M_{s*} << 1$;

$$M_*(x_*, t_*) = 2\left(\frac{\alpha}{\beta + \lambda_*}\right) \exp\left[-\frac{x_* D_*}{U_*}\left(\frac{4\alpha}{D_*} + \lambda_*\right)\right] G\left(\sqrt{\xi}, \sqrt{Z}\right) \quad [18]$$

$$\bar{N}_*(x_*, t_*) = \exp\left[-\frac{x_* D_*}{U_*}\left(\frac{4\alpha}{D_*} + \lambda_*\right)\right]\left[2G\left(\sqrt{\xi}, \sqrt{Z}\right) \exp(-Z)\, I_o\left(\sqrt{4\xi Z}\right)\right] , \quad [19]$$

in which

$$\alpha = \sigma Kr_* h_*/(h_* + \sigma Kr_*) \ ,$$

$$\beta = \theta_* h_*/(h_* + \sigma Kr_*) \ ,$$

$$\xi = \left(\frac{4\alpha\beta}{\beta + \lambda_*}\right)(x_*/U_*) \ ,$$

$$Z = (\beta_* + \lambda_*)(t_* - x_* D_*/U_*) \ ,$$

I_o is the zeroth order Bessel Function with a purely imaginary argument, and

$$G(p,q) = \int_o^q \phi\, e^{-\phi^2} I_o(2p\phi)\, d\phi \ .$$

Equations 18 and 19 were programmed for numerical solution on the CDC 1604-A digital computer and solutions were obtained for a systematic variation of the parameters (Figs. 1a through 1e). The program was also used to compare the model with experimental results for low levels of deposition.

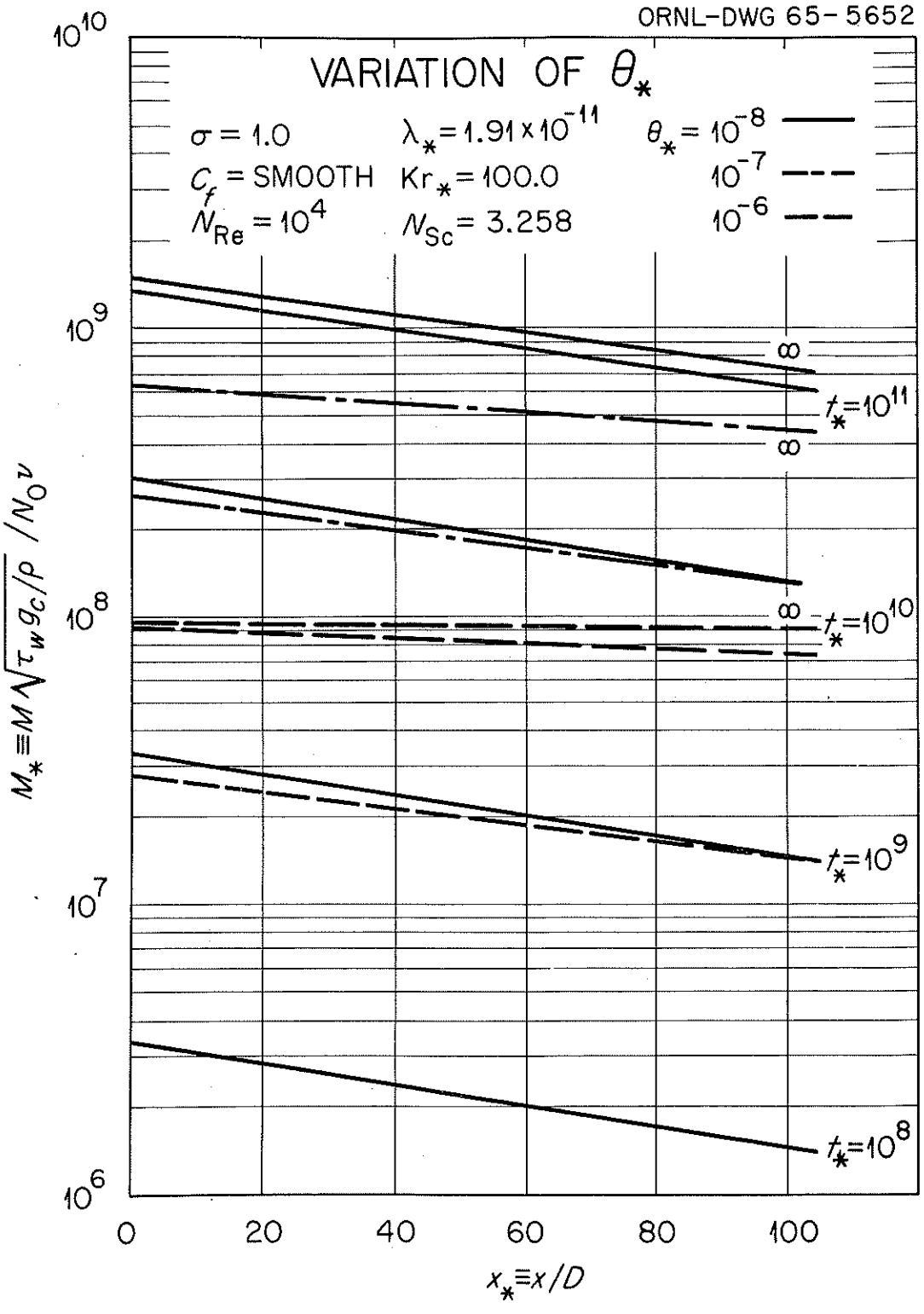

Fig. 1(a) Variation of Fission-Product Deposition Parameters.

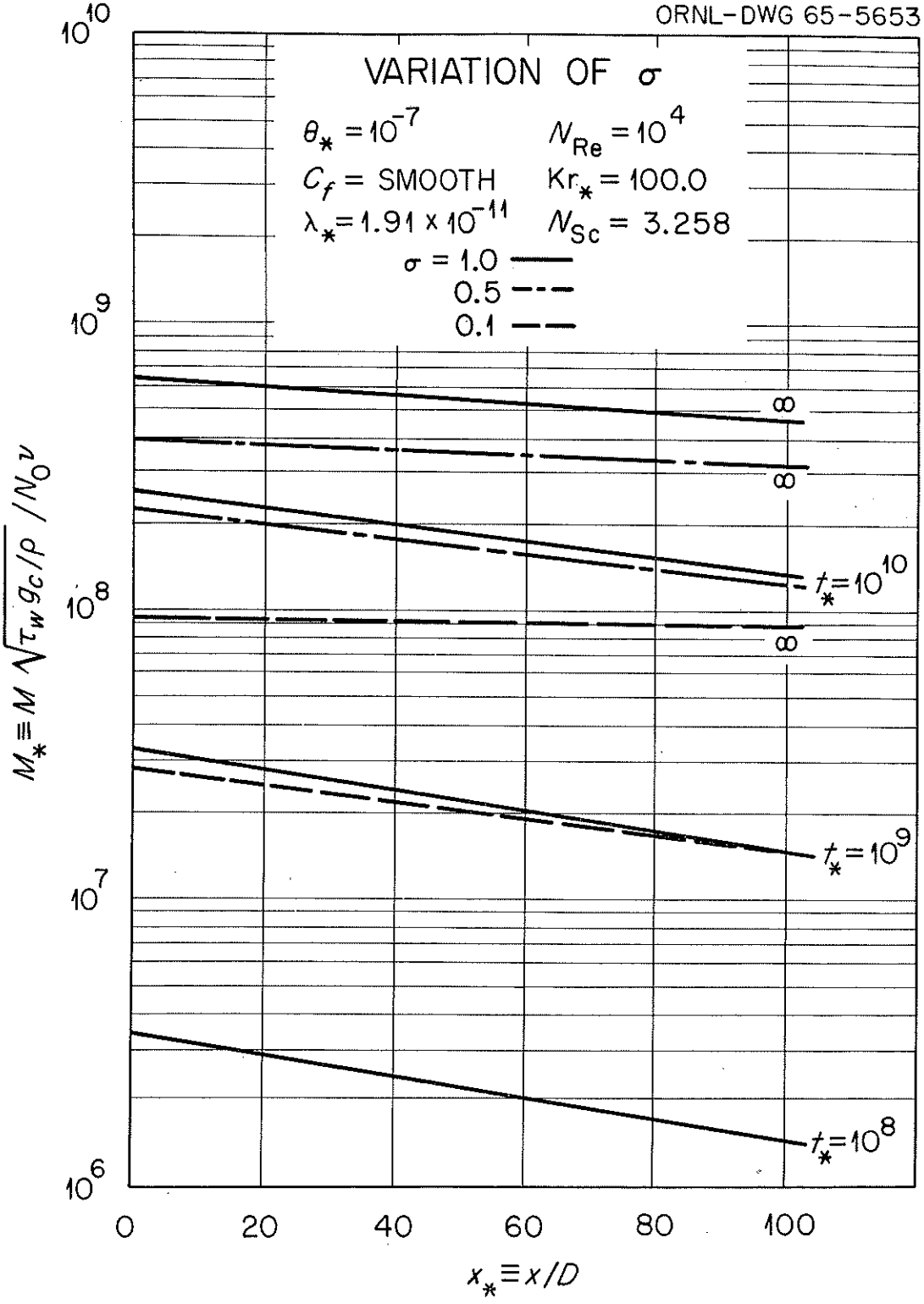

Fig. 1(b) Variation of Fission-Product Deposition Parameters

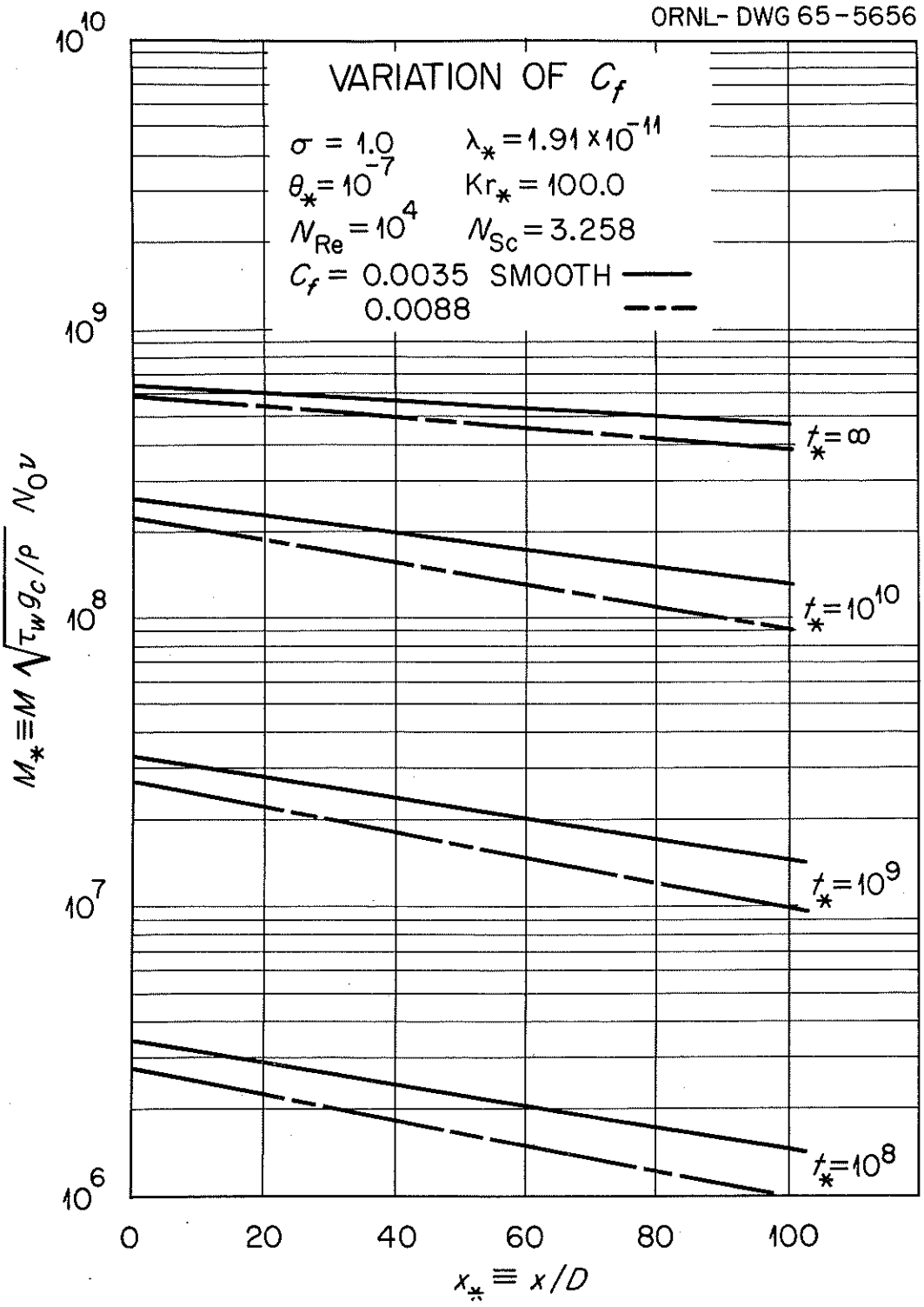

Fig. 1(c) Variation of Fission-Product Deposition Parameters

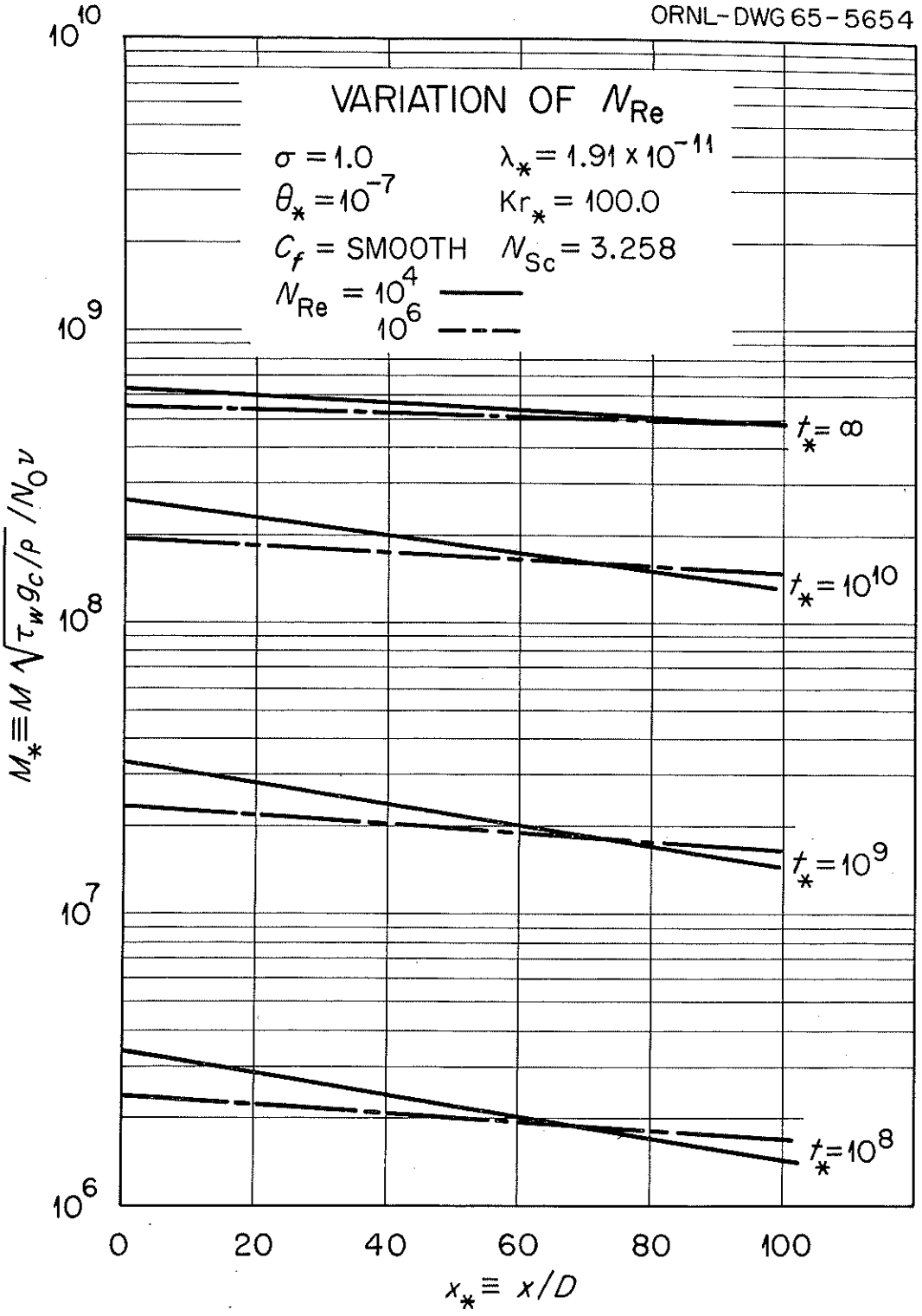

Fig. 1(d) Variation of Fission-Product Deposition Parameters

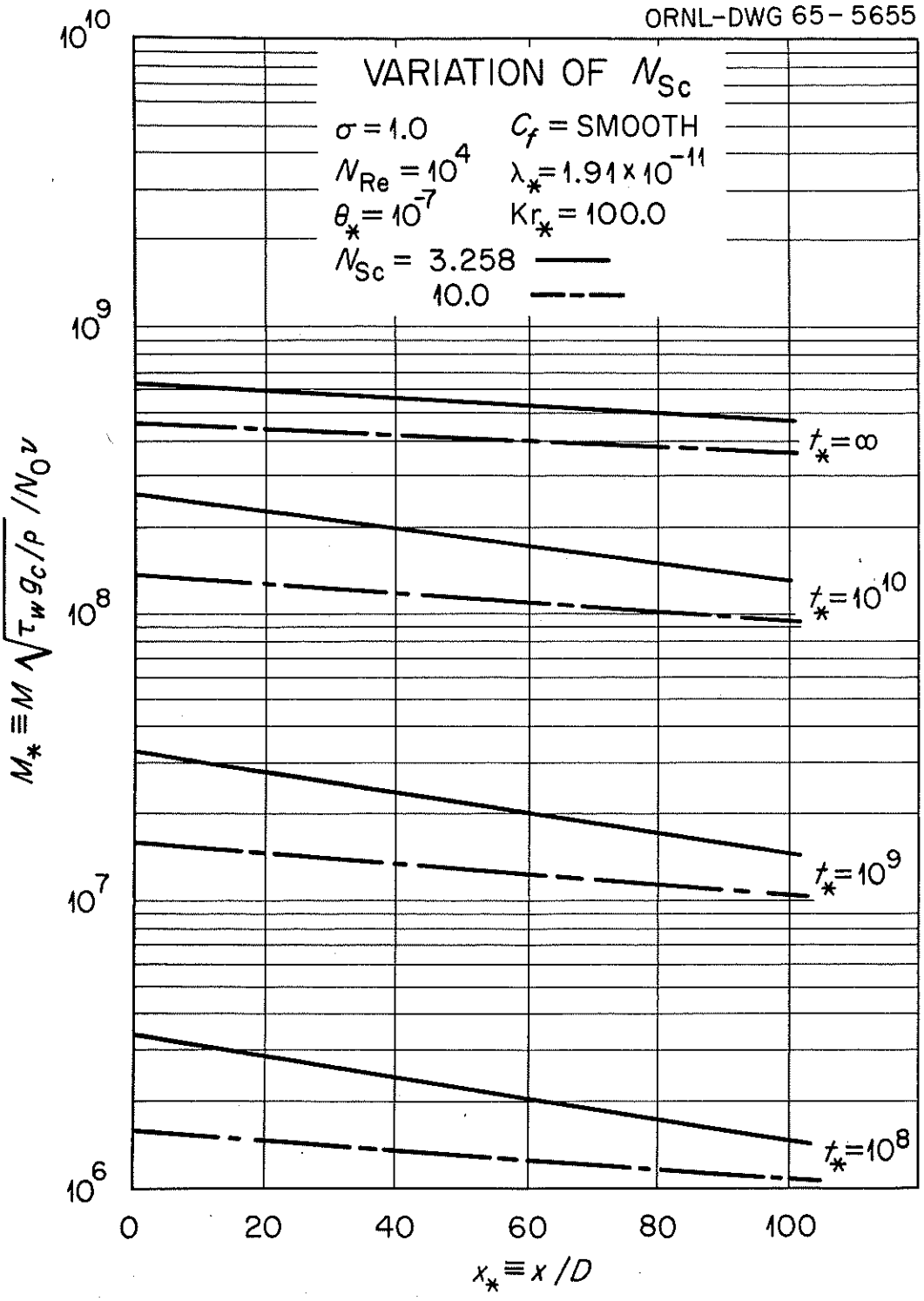

Fig. 1(e) Variation of Fission-Product Deposition Parameters

EXPERIMENTAL RESULTS

Observations of iodine transported through a turbulently flowing helium stream and deposited onto stainless and carbon steel conduit were made with the experimental apparatus shown in Fig. 2. The closed circuit was held essentially isothermal at 500°F by "clamp-on" heaters downstream of the circulator, and by piping insulation.

The deposition area was 12 ft of nominally 1-in.-diam pipe attached at the ends to the remainder of the loop by mechanical joints. A small sample of PaI_2, tagged with a known ratio of ^{131}I to ^{127}I, was heated at a constant temperature (up to 800°F) in an appended chamber. After dissociating, the iodine diffused into the helium stream through a connecting tube immediately upstream of the deposition area. Recirculation of the injected iodine was inhibited by a silver-wire filter downstream of the deposition area. An average injection rate was determined by timing the injection period and counting the sample before and after each test. The ratio of ^{131}I to ^{127}I for the deposited iodine was assumed to be the same as the original source--(confirmed to be in good agreement by neutron activation analyses of solutions leached from the deposition surface). The amount and distribution of the deposited iodine was determined by scanning with a scintillation type detector mounted on a track underneath the deposition area. Calibration was obtained by comparing scan results with radiochemical analysis of the surface. Figure 3 is a typical run in which results of the scan, radiochemical analysis, and neutron activation analysis are compared to show their agreement.

Experiments from the present apparatus were conducted with ^{127}I on stainless and mild steel at 500°F. Desorption experiments were made to

PHOTO 71170A

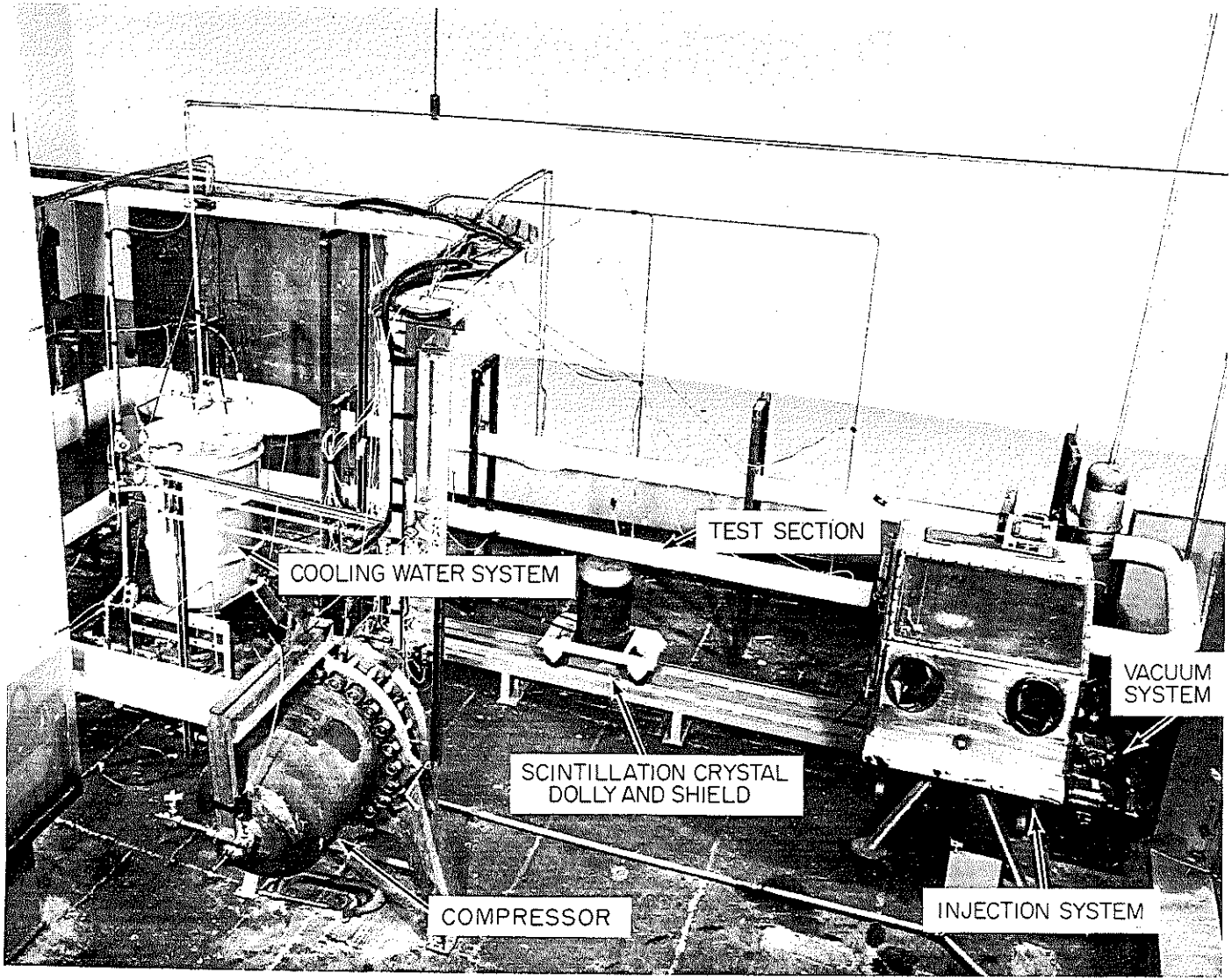

Fig. 2 Fission-Product Deposition Test Facility

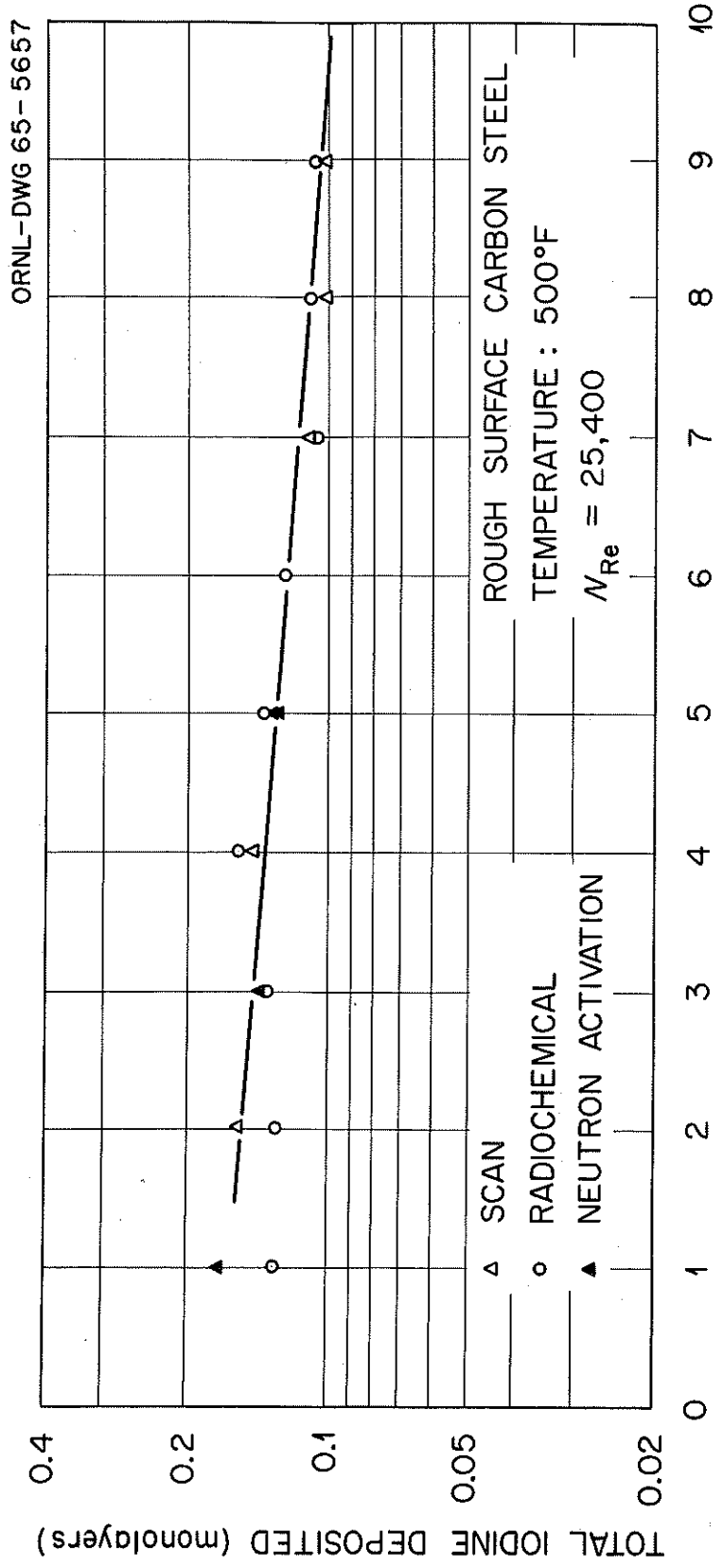

Fig. 3. Comparison of Deposition Measurements by Radiochemical Analysis, Scanning, and Neutron Activation

check the basic assumption represented in Eq. 1. In these experiments, deposition was carried to a low level and then discontinued by rapidly cooling the source. Circulation of the helium was continued at 500°F and the scintillation counter held at a fixed position about two feet downstream from the source to observe the decrease in activity with time. Typical results for type 316 stainless steel are shown on Fig. 4. Such desorption curves tend to approach an apparent equilibrium value but not necessarily the same for each experiment. If the measured concentration at each time is reduced by the equilibrium amount, a curve is obtained that follows Eq. 1; and the slope gives an experimental value for θ. Figure 5 shows the data for several desorption runs plotted in this manner. From the slope, $\theta \cong 2.5 \times 10^{-4}$ sec^{-1} for iodine on stainless steel at 500°F. For iodine on mild steel at 500°F, θ was determined in the same manner to be $\sim 2.0 \times 10^{-7}$ sec^{-1}.

The surface concentration limit, M_S, was determined by injecting until equilibrium was reached under conditions where $\frac{\theta_* M_*}{\sigma K r_*} << 1.0$. Under these conditions, Eq. 15 reduces to $M_{S*} = M_*$, or $M_S = M$. For iodine on smooth stainless steel tubing, $M_S \cong .04$ $\mu g/cm^2$ (~ 0.12 monolayers of geometrical surface). A similar test gave $M_S \cong 0.76$ $\mu g/cm^2$ (~ 2.3 monolayers) for mild steel tubing. These values have not been verified yet by a sufficiently large number of runs under many operating conditions. The basic surface chemistry must be more firmly established.

Using the above measured values, low-level non-saturated, ($\frac{M_*}{M_S} << 1$), deposited ^{127}I on stainless steel was predicted and compared with experiment in Fig. 6.

Transient adsorption of iodine on mild steel was obtained in a "multi-injection" experiment in which the iodine was injected in specific increments. After each incremental injection, the source and deposition region were cooled

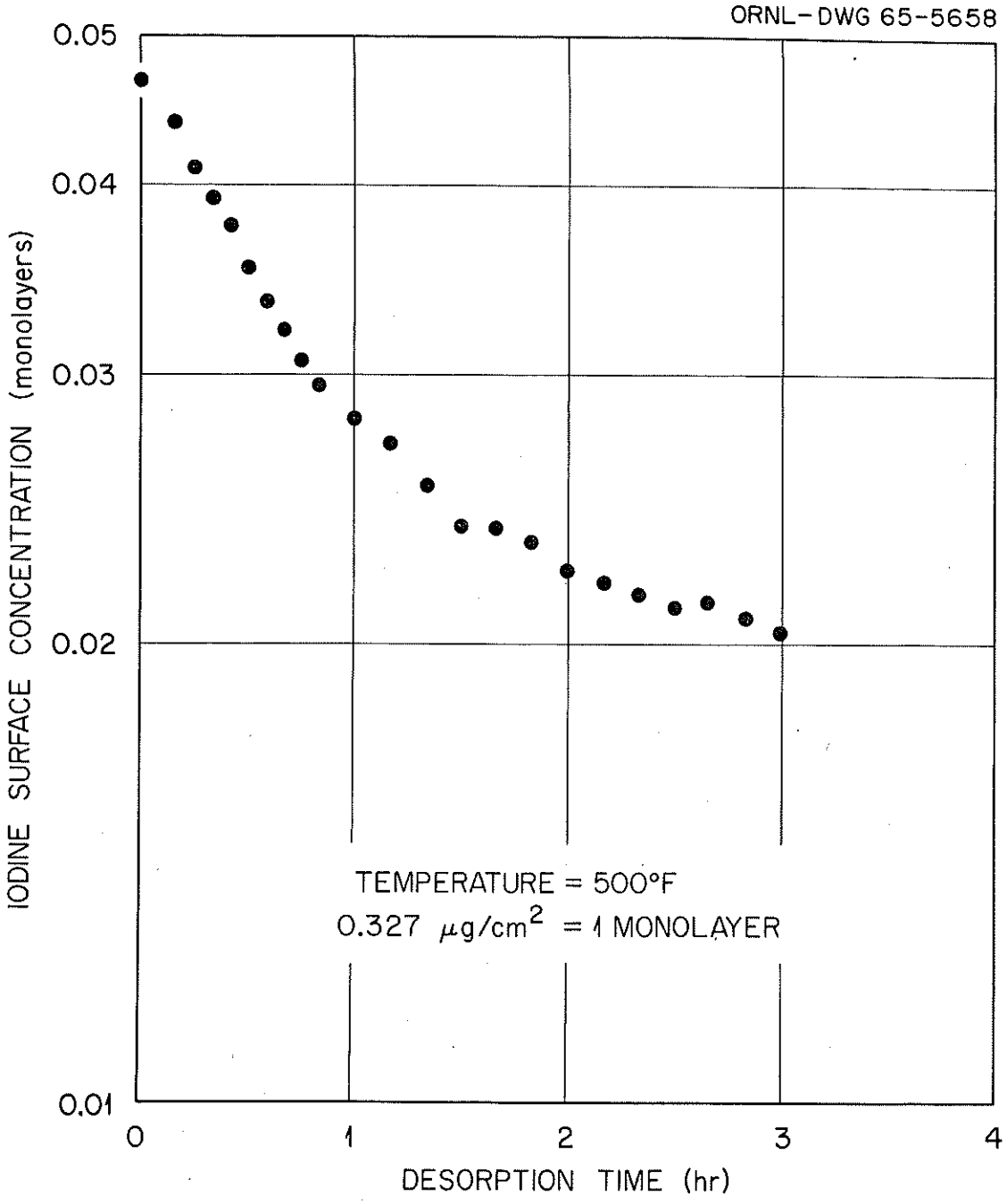

Fig. 4. Desorption of ^{127}I from Stainless Steel at 500°F

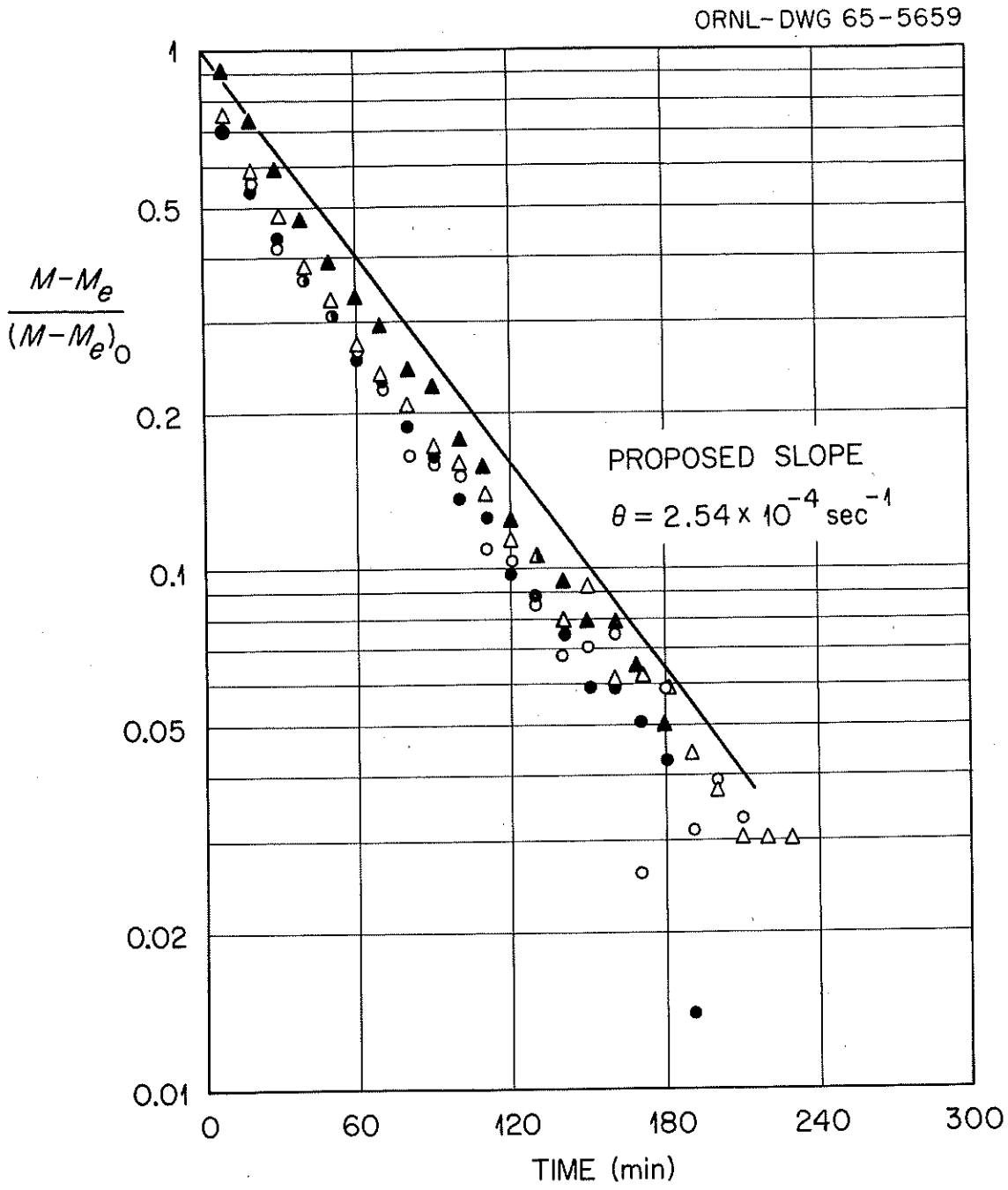

Fig. 5. Desorption of ^{127}I from Stainless Steel at 500°F, Adjusted for Equilibrium

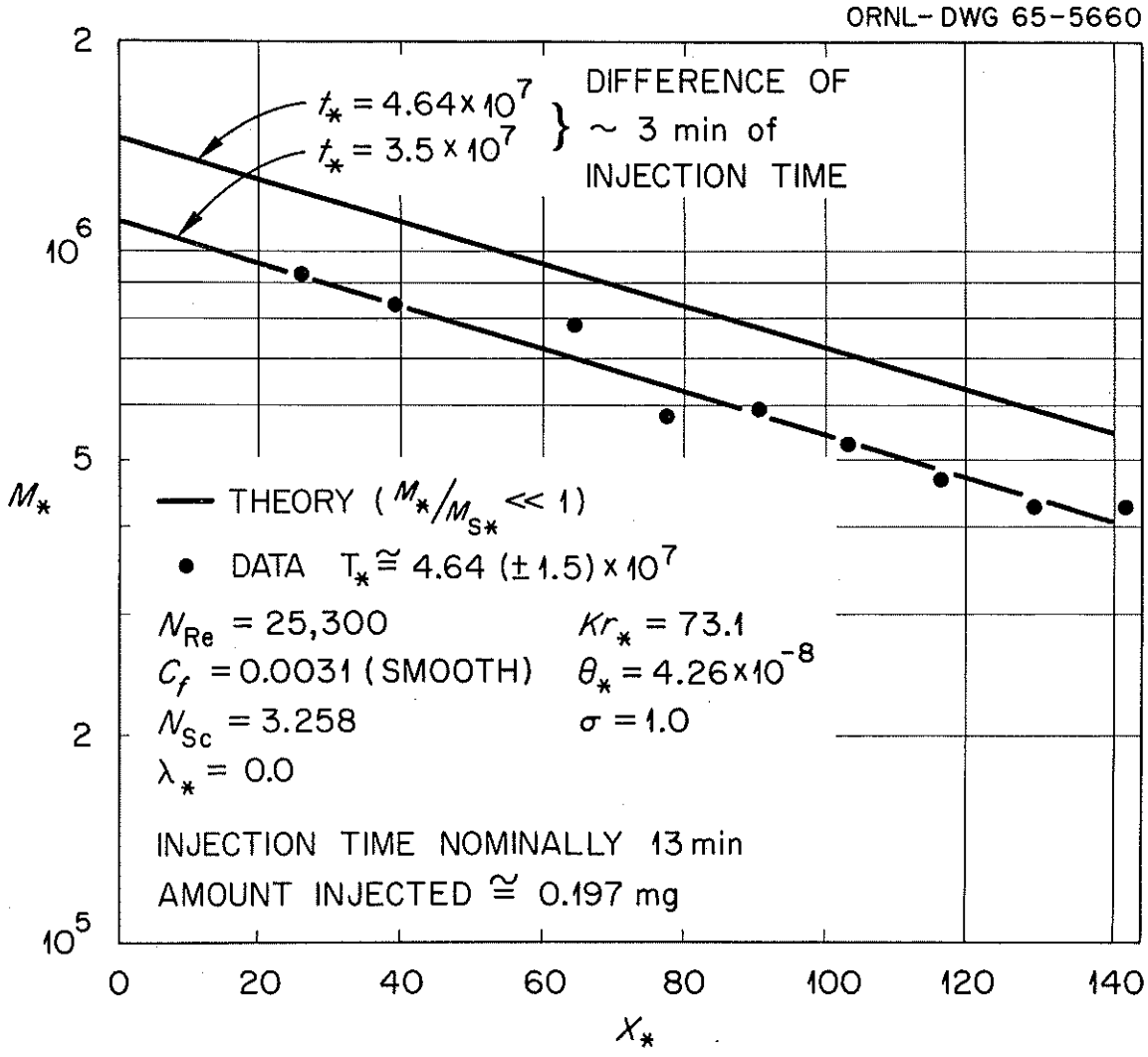

Fig. 6. Deposition of ^{127}I on Stainless Steel at 500°F, Nonequilibrium ($M_*/M_{S*} \ll 1$).

rapidly to inhibit desorption and further injection, and the source counted to determine the amount injected. After scanning to determine the deposition level, the test section was brought back to the operating temperature (500°F) rapidly and the next injection increment started. The results compared with the predictions at low-levels are shown in Fig. 7. The lower three curves were at injection rates significantly lower than for the other curves. To compare on a consistent basis, low levels of deposition can be assumed approximately proportional to t/N_o (see Figs. 1a through 1e).

DISCUSSION AND CONCLUSIONS

The model presented assumed validity of the heat-mass analogy under conditions of radioactive decay and surface saturation, postulates the surface reaction, and correlates the transport and deposition of fission products. Qualitative agreement with the model for deposition of stable ^{127}I on mild steel is apparent in the progressive decrease in slope as equilibrium is approached (Fig. 7). The slopes of the curves are in good agreement with the theory for low coverage (Eq. 18), although the data are slightly lower. This was expected because no credit was taken for the higher rate of concentration depletion in the entrance region.

The results indicate that the study of fission-product deposition involves the same problems inherent in the many physical adsorption isotherms (9) and chemisorption surface reactions (8) of stable species. The transport behavior seems to be important only for short-lived isotopes and non-equilibrium levels of deposition. To fully predict fission product deposition, the chemical form and reaction with a given surface which may contain previously deposited molecules must be determined. If the reaction

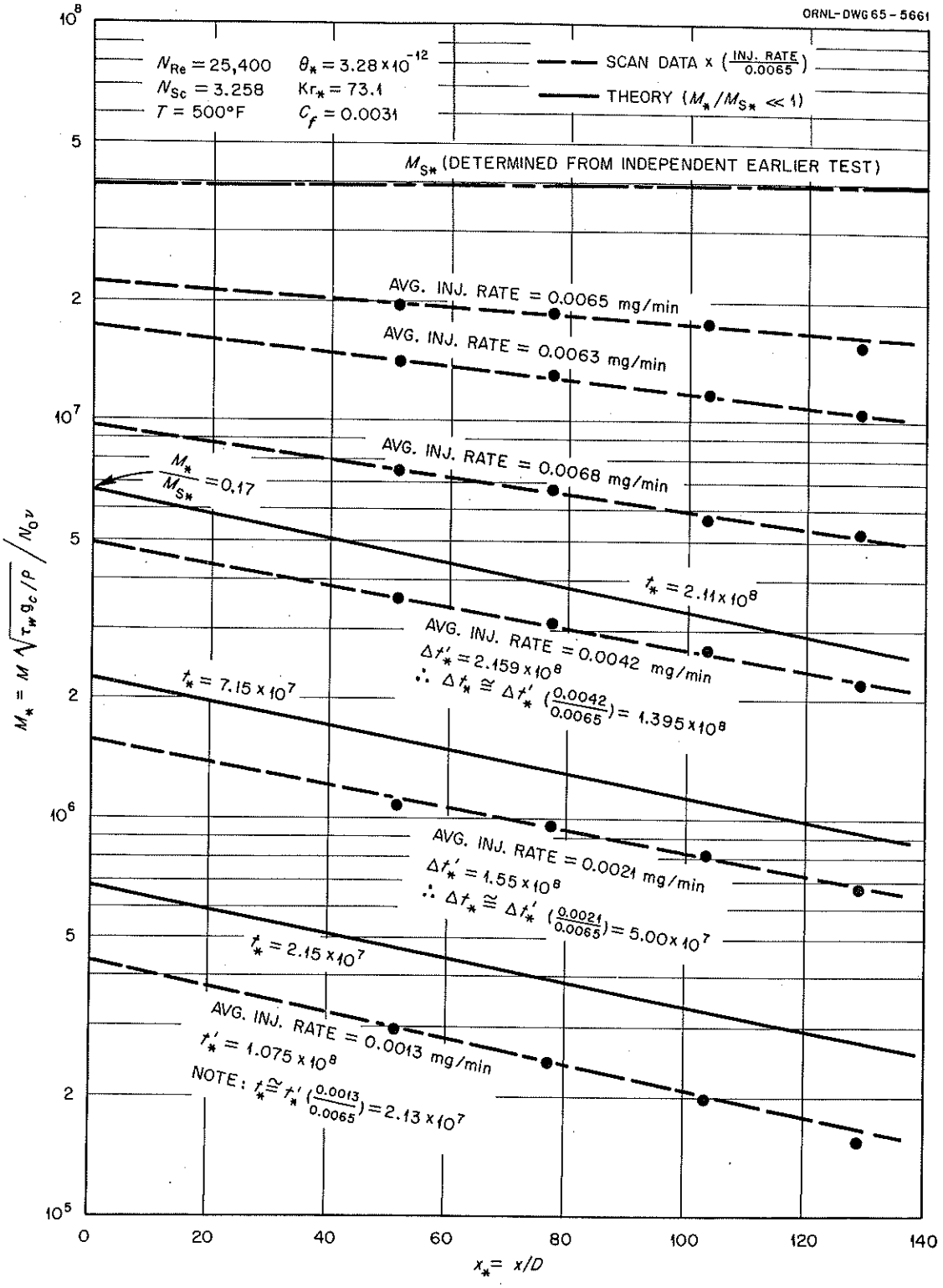

Fig. 7. Transient Deposition of ^{127}I on Mild Steel at 500°F, Comparison of Theory and Experiment

is an interchange process that can be described by an equation of the Arrhenium type, then complete characterization may only require determining values for the activation energy, Q, the vibrational period, ω, the active surface fraction, σ, and the saturation level of adsorption, M_S. These parameters may be functions of the treatment of the surface material, state of oxidation, temperature, previous surface coverage, and other variables. The need for further investigation is indicated in which static tests may be used to characterize surface reactions for the more important fission products.

NOMENCLATURE

C_f = Friction coefficient

C_{fo} = Friction coefficient for smooth tubing

D = Conduit equivalent diameter

g_c = Proportionality constant

h = Mass transfer coefficient

Kr = Gross collision rate term = $(RTg_c/2\pi m)^{1/2}$

m = Molecular weight of the fission-product

M = Fission-product concentration on the conduit surface

M_s = Saturation limit of fission product surface concentration

$\bar{N}_\delta$ = Fission-product concentration in the gas stream at the conduit surface

$\bar{N}$ = Radial average of fission-product concentration in the gas stream

$\bar{N}_o$ = $\bar{N}$ at the source ($x = 0$)

N_{Re} = Reynolds number

N_{Sc} = Schmidt number

p = Fission-product partial pressure near the conduit surface

Q = Heat of vaporization (activation energy)

R = Universal gas constant

t = Time coordinant

T = Absolute temperature

$\bar{U}_x$ = Bulk mean axial velocity

x = Axial distance coordinant

δ = Thickness of desorption region

θ = Fractional desorption rate term defined by Eq. 2

λ = Fission-product decay constant

μ = Carrier stream viscosity

ν = Carrier stream kinematic viscosity ($= \frac{\mu}{\rho}$)

ρ = Carrier stream density

σ = Fraction of those molecules stricking bare surface that become adsorbed

τ_w = Wall shearing stress

ω = Period of vibration of the adsorbed molecules

BIBLIOGRAPHY

1. M. N. Ozisik, "An Analytical Model for Fission Product Transport and Deposition from Gas Streams," USAEC Report ORNL-3379, Oak Ridge National Laboratory, July 1963.

2. M. N. Ozisik, "A Transient Analysis of Fission Product Deposition," USAEC Report ORNL-TM-650, Oak Ridge National Laboratory, October 1963.

3. M. N. Ozisik, "Effects of Temperature on Fission Product Deposition," USAEC Report ORNL-3542, Oak Ridge National Laboratory, March 1964.

4. J. T. Beard, R. A. Hollister, and T. S. Kress, "A Code for Computing the Rate of Fission Product Deposition from a Gas Stream,: USAEC Report ORNL-TM-723, Oak Ridge National Laboratory, March 1964.

5. G. E. Raines, A. Abriss, D. L. Morrison, and R. A. Ewing, "Experimental and Theoretical Studies of Fission Product Deposition in Flowing Helium," USAEC Report BMI-1688, Battelle Memorial Institute, August 1964.

6. F. H. Neill, D. M. Eissenberg, and D. L. Gray, "Iodine Transport and Deposition in a High-Temperature, Helium Loop - First Test Series," USAEC Report ORNL-TM-1134, Oak Ridge National Laboratory, To be published.

7. T. S. Kress, Analytical Model for Fission Product Deposition, "GCRP Semiann. Prog. Rep. July 1964," USAEC Report ORNL-3619, Oak Ridge National Laboratory, July 1964, pp. 101-102.

8. M. J. D. Low, "Kinetics of Chemisorption of Gases on Solids," Reprinted from June, 1960 issue of Chemical Reviews published by the Americal Chemical Society.

9. W. Adamson, Physical Chemistry of Surfaces, Interscience Publishers, Inc., New York, 1960, Chapt. XI.

10. B. M. W. Trapnell, Chemisorption, Academic Press, Inc., New York, 1955, Chapt. IV & V.

11. J. O. Hinze, Turbulence, McGraw Hall Book Company, Inc., New York, 1959, p. 556.

12. L. F. Epstein and T. F. Evans, "Deposition of Matter from a Flowing Stream," GEAP-4140, December 1, 1962, General Electric Company, Vallecitos Atomic Laboratory.

13. H. S. Carslaw and J. C. Jaeger, Conduction of Heat in Solids, 2nd.Ed., Clarendon Press, Oxford, 1959, pp. 391-394.

APPENDIX

Equilibrium Solution

Consider Eqs. 3, 4 and 5 in nondimensional form:

$$\frac{\partial \bar{N}_*}{\partial t_*} + \frac{1}{C_f N_{Re}} \frac{\partial \bar{N}_*}{\partial x_*} + \lambda_* \bar{N}_* + \frac{4h_*}{\sqrt{C_f N_{Re}}} (\bar{N}_* - \bar{N}_{\delta *}) = 0 , \qquad [A\text{-}1]$$

$$\sqrt{C_f}\, N_{Re}\, \delta_* \left[\frac{\partial \bar{N}_{\delta *}}{\partial t_*} + \lambda_* \bar{N}_{\delta *}\right] - h_*(\bar{N}_* - \bar{N}_{\delta *}) - \theta_* M_* + \sigma Kr_* \bar{N}_{\delta *}(1 - M_*/M_{s*}) = 0 , \qquad [A\text{-}2]$$

and

$$\frac{\partial M_*}{\partial t_*} - \sigma \bar{N}_{\delta *} Kr_* (1 - M_*/M_{s*}) + M_* (\theta_* + \lambda_*) = 0 . \qquad [A\text{-}3]$$

At equilibrium, $\frac{\partial \bar{N}_*}{\partial t_*} = \frac{\partial \bar{N}_{\delta *}}{\partial t_*} = \frac{\partial M_*}{\partial t_*} = 0$.

Therefore from A-3

$$M_* = \frac{\sigma Kr_* \bar{N}_{\delta *}}{\left[\theta_* + \lambda_* + \frac{\sigma Kr_*}{M_{s*}} \bar{N}_{\delta *}\right]} . \qquad [A\text{-}4]$$

Substituting into A-2 gives

$$\bar{N}_* = \frac{A\bar{N}_{\delta *} + B\bar{N}_{\delta *}^2}{C + D\bar{N}_{\delta *}} , \qquad [A\text{-}5]$$

where $A = M_{s*} \left[(\theta_* + \lambda_*)(\sqrt{C_f} N_{Re}\, \delta_* \lambda_* + h_* + \sigma Kr_*) - \theta_* \sigma Kr_*\right]$,

$B = \sigma Kr_* (\sqrt{C_f} N_{Re}\, \delta_* \lambda_* + h_*)$,

$C = M_{s*}\, h_* (\theta_* + \lambda_*)$, and

$D = h_*\, \sigma Kr_*$.

Differentiating A-5 gives

$$\frac{\partial \bar{N}_*}{\partial x_*} = \frac{\partial \bar{N}_{\delta *}}{\partial x_*} \frac{2BC(\bar{N}_{\delta *}) + BD(\bar{N}^2_{\delta *}) + AC}{(C + D\bar{N}_\delta)^2} \quad . \qquad [A\text{-}6]$$

Substituting A-6 and A-5 into A-1, multiplying by $C_f N_{Re}(C + D\,\bar{N}_{\delta *})^2$ and rearranging gives

$$\frac{\partial \bar{N}_*}{\partial x_*}\left[BD\,\bar{N}^2_{\delta *} + 2BC\,\bar{N}_{\delta *} + AC\right] + \bar{N}_{\delta *}\,(C + D\,\bar{N}_{\delta *})\,(F + G\,\bar{N}_{\delta *}) = 0 \ ,$$

where $F = C_f N_{Re}\,\lambda_* A + 4\sqrt{C_f}\,h_*\,(A - C)$,

and $G = C_f N_{Re}\,\lambda_* B + 4\sqrt{C_f}\,h_*\,(B - D)$.

Integrating gives

$$\int_{\bar{N}_{\delta *o}}^{\bar{N}_{\delta *}} \frac{BD\,\bar{N}^2_{\delta *} + 2BC\,\bar{N}_{\delta *} + AC}{\bar{N}_{\delta *}\,(C + D\,N_{\delta *})\,(F + G\,\bar{N}_{\delta *})}\, d\bar{N}_{\delta *} = -\int_o^x dx \ ,$$

or

$$\int_{\bar{N}_{\delta *o}}^{\bar{N}_{\delta *}} \left[\frac{C_1}{\bar{N}_{\delta *}} + \frac{C_2}{C + D\,\bar{N}_{\delta *}} + \frac{C_3}{F + G\,\bar{N}_{\delta *}}\right] d\bar{N}_{\delta *} = -\int_o^x dx \ ,$$

which integrates to

$$C_1 \ln \bar{N}_{\delta *}\Big|_{\bar{N}_{\delta *o}}^{\bar{N}_{\delta *}} + \frac{C_2}{D} \ln (C + D\,\bar{N}_{\delta *})\Big|_{\bar{N}_{\delta *o}}^{\bar{N}_{\delta *}}$$

$$+ \frac{C_3}{G} \ln (F + G\,\bar{N}_{\delta *})\Big|_{\bar{N}_{\delta *o}}^{\bar{N}_{\delta *}} = -x \ , \qquad A\text{-}7$$

where $\bar{N}_{\delta *}$ and $\bar{N}_{\delta *o}$ can be found from A-5 ($\bar{N}_{*o} = 1$) ,

$$C_1 = \frac{A}{F} \ , \quad C_2 = \frac{BCD - AD^2}{FD - CG} \ , \text{ and}$$

$$C_3 = \frac{2BCG - ACG^2/F - BDE}{CG - DF} \ .$$

For the equilibrium solution to Eqs. 9 and 10, set $\delta_* = 0$ in Eq. A-7 and solve A-4 for M_*.

Internal Distribution

1. S. E. Beall
2. F. L. Culler
3. A. P. Fraas
4. P. N. Haubenreich
5-155. T. S. Kress
156. M. I. Lundin
157. R. N. Lyon
158. H. C. McCurdy
159. A. J. Miller
160. F. H. Neill
161. A. M. Perry
162. H. W. Savage
163. A. W. Savolainen
164. M. J. Skinner
165. I. Spiewak
166. D. B. Trauger
167. G. D. Whitman
168-169. Central Research Library (CRL)
170-171. Y-12 Document Reference Section (DRS)
172-174. Laboratory Records Department (LRD)
175. Laboratory Records Department - Record Copy (LRD-RC)

External Distribution

176-191. Division of Technical Information Extension (DTIE)
192. Research and Development Division, ORO
193-194. Reactor Division, ORO